

## ORIGINAL ARTICLE

# Diversification of circulating and tumor-infiltrating plasmacytoid DCs towards the P3 (CD80<sup>+</sup> PDL1<sup>-</sup>)-pDC subset negatively correlated with clinical outcomes in melanoma patients

Eleonora Sosa Cuevas<sup>1,2</sup> , Nathalie Bendriss-Vermare<sup>3</sup> , Stephane Mouret<sup>4</sup>,  
Florence De Fraipont<sup>5</sup>, Julie Charles<sup>1,4</sup>, Jenny Valladeau-Guilemond<sup>3</sup>, Laurence Chaperot<sup>1,2</sup> &  
Caroline Aspod<sup>1,2</sup> 

<sup>1</sup>Institute for Advanced Biosciences, Immunobiology and Immunotherapy in Chronic Diseases, Inserm U 1209, CNRS, UMR 5309, Université Grenoble Alpes, Grenoble, France

<sup>2</sup>Etablissement Français du Sang Auvergne-Rhône-Alpes, R&D Laboratory, Grenoble, France

<sup>3</sup>Univ Lyon, Université Claude Bernard Lyon 1, INSERM 1052, CNRS 5286, Centre Léon Bérard, Centre de Recherche en Cancérologie de Lyon, Lyon, France

<sup>4</sup>Dermatology Clinic, Grenoble University Hospital, Grenoble, France

<sup>5</sup>Medical Unit of Molecular Genetic (Hereditary Diseases and Oncology), Grenoble University Hospital, Grenoble, France

## Correspondence

C Aspod, EFS-R&D Laboratory,  
EMR EFS-UGA-INSERM U1209- CNRS,  
29 avenue du Maquis Gresivaudan,  
38700 La Tronche, France.  
E-mail: Caroline.Aspod@efs.sante.fr

Received 12 April 2021;  
Revised 7 March 2022;  
Accepted 9 March 2022

doi: 10.1002/cti2.1382

*Clinical & Translational Immunology*  
2022; 11: e1382

## Abstract

**Objectives.** Plasmacytoid DCs (pDCs) play a critical yet enigmatic role in antitumor immunity through their pleiotropic immunomodulatory functions. Despite proof of pDC diversity in several physiological or pathological contexts, pDCs have been studied as a whole population so far in cancer. The assessment of individual pDC subsets is needed to fully grasp their involvement in cancer immunity, especially in melanoma where pDC subsets are largely unknown and remain to be uncovered. **Methods.** We explored for the first time the features of diverse circulating and tumor-infiltrating pDC subsets in melanoma patients using multi-parametric flow cytometry, and assessed their clinical relevance. Based on CD80, PDL1, CD2, LAG3 and Axl markers, we provided an integrated overview of the frequency, basal activation status and functional features of pDC subsets in melanoma patients together with their relationship to clinical outcome. **Results.** Strikingly, we demonstrated that P3-pDCs (CD80<sup>+</sup>PDL1<sup>-</sup>) accumulated within the tumor of melanoma patients and negatively correlated with clinical outcomes. The basal activation status, diversification towards P1-/P2-/P3-pDCs and functionality of several pDC subsets upon TLR7/TLR9 triggering were perturbed in melanoma patients, and were differentially linked to clinical outcome. **Conclusion.** Our study shed light for the first time on the phenotypic and functional heterogeneity of pDCs in the blood and tumor of melanoma patients and their potential involvement in shaping clinical outcomes. Such novelty brightens our understanding of pDC complexity, and prompts the further deciphering of pDCs' features to better apprehend and exploit these potent immune

players. It highlights the importance of considering pDC diversity when developing pDC-based therapeutic strategies to ensure optimal clinical success.

**Keywords:** clinical outcome, immune subversion, melanoma, pDC subsets

## INTRODUCTION

Dendritic cells (DCs) are crucial immune cells that intertwine innate and adaptive immunity after pathogen or danger recognition and subsequently trigger appropriate and controlled immune responses.<sup>1–3</sup> BDCA2<sup>+</sup> plasmacytoid DCs (pDCs), representing 0.2–0.8% of peripheral blood mononuclear cells (PBMCs) in healthy donors (HDs), are portrayed as major actors in antiviral immunity given their massive type I interferon (IFN) production after TLR7/TLR9 stimulation.<sup>4–7</sup> Nonetheless, they also play a rather puzzling role in antitumor immunity through their pleiotropic immunomodulatory functions.<sup>8,9</sup> Indeed, pDCs can induce potent antitumor cytotoxic responses through antigen cross-presentation to T cells<sup>10,11</sup> or secretion of pro-inflammatory cytokines. However, tumor-derived soluble factors (PGE2, IL-10, TGF- $\beta$ ) or LAG-3-dependent pDC activation can suppress type I IFN production,<sup>12–14</sup> whereas pDC's hijacking by tumor cells subsequently induced pro-tumoral regulatory and Th2 immune responses which contribute to the establishment of an immunosuppressive tumor microenvironment.<sup>15–20</sup> Likewise, in melanoma patients, the accumulation of tumor-infiltrating pDCs was linked to a bad prognosis<sup>12,15,21,22</sup> and pDCs accumulated in draining lymph nodes were shown to have an impaired IFN $\alpha$  secretion.<sup>23,24</sup> Yet, tumor antigen-loaded pDCs isolated from patient's blood can be vectors for immunotherapy after proper activation *ex vivo* and elicit favorable antitumor immune responses in patients upon vaccination.<sup>11,25</sup> Given their unique environmental plasticity and strengths, elucidating how to permanently regain functionality of pDCs that have been negatively reprogrammed by tumor cells remains of the utmost importance for future immunotherapeutic developments.

Human pDCs have been mostly studied as a whole, even though heterogeneity of this DC subset has been suggested in several studies, both at steady-state and upon TLR stimulation, and under normal or pathologic contexts. In HDs, the

expression of CD2, CD5, CD81 and Axl distinguishes several pDC subsets with distinct phenotypes and functions.<sup>26–28</sup> Distinct pDC subsets have also been identified in mice using several markers such as CD9, SiglecH and CXCL10.<sup>29–31</sup> Later on, multiparametric phenotypic characterisation and unbiased single-cell RNA sequencing of human blood and tonsils samples identified a contamination of the pDC gate (CD45<sup>+</sup>Lin<sup>-</sup>HLA-DR<sup>+</sup>BDCA2<sup>+</sup>) by a closely related DC precursor population (AS DCs) expressing CD2, CD5 and Axl,<sup>32–34</sup> which are counterparts of the transitional DC (tDC) described in mice.<sup>35</sup> After TLR triggering, AS DCs could produce IL12p40 but low IFN $\alpha$ , induce T-cell proliferation, and potentially differentiate into conventional DCs.<sup>32,33</sup> These findings lead to believe that previously described pDC subsets (mainly CD2<sup>hi</sup> pDCs) were in part DC precursors mixed within “pure” pDCs and that some of the functionalities already granted to pDCs were actually because of contamination by AS DCs.<sup>34</sup> Specific pDC subsets have also been uncovered in different physiological or malignant contexts. Neonates were shown to possess an extended CD2<sup>+</sup> pDC compartment than adults without affecting type I IFN response, and a CD2<sup>+</sup>CD5<sup>+</sup> pDC subpopulation responsible for IL-12p40 production was also identified.<sup>28</sup> After human skin wounding, a CD1a-bearing BDCA2<sup>+</sup>CD123<sup>int</sup> pDC subset was shown to rapidly infiltrate the skin and contribute to acute sterile inflammation.<sup>36</sup> Blood CD2<sup>low</sup> pDCs were also preferentially depleted in HIV-infected patients.<sup>37</sup> Interestingly, heterogeneity of pDCs was also observed in cancer where a LAG3<sup>+</sup>pDC subset (representing 6% of total circulating pDCs) was found enriched at tumor sites of melanoma patients and partly responsible for driving an immune-suppressive environment.<sup>13</sup> The activation of LAG3<sup>+</sup> pDCs was TLR-independent and triggered high IL6 secretion. Strikingly, after excluding AS DCs from their analysis, Alculumbre *et al.* proved that activation of human pDCs with a single TLR-L stimulus triggered cell diversification into three stable subpopulations.<sup>38</sup> Defined by the combination of PDL1 and CD80 expression, specific

subpopulations of pDCs were phenotypically and functionally distinct. PDL1<sup>+</sup>CD80<sup>-</sup> pDCs (P1-pDCs) specialised in type I IFN and IL6 production, PDL1<sup>-</sup>CD80<sup>+</sup> pDCs (P3-pDCs) promoted T-cell activation and Th2 differentiation, whereas PDL1<sup>+</sup>CD80<sup>+</sup> pDCs (P2-pDCs) displayed both innate and adaptive functions. Interestingly, the dysregulation of these subsets has been described in autoimmune diseases: P1-pDCs were detected in samples (blood or skin) from patients with psoriasis or lupus.<sup>38</sup> Furthermore, human pDCs efficiently diversified into functional P1-, P2- and P3-pDC effector subsets in response to SARS-CoV-2.<sup>39</sup>

In cancer, especially in melanoma, pDC subsets are largely unknown and remain to be uncovered. Given the unique role played by each pDC subset and their differential enrichment in diverse pathologic settings, their analysis in the context of cancer could help better understand pDC pathophysiology and elucidate tumor escape from immune control. In this study, we explored for the first time the features of diverse circulating and tumor-infiltrating pDC subsets in melanoma patients using multi-parametric flow cytometry. We investigated in blood and tumor infiltrates the frequency, the basal activation status together with the functionality of pDC subsets and assessed their clinical relevance. We also characterised the interrelations within pDC subsets that associated with clinical outcomes. Our work highlighted the diversity of pDC subsets in blood and tumor of melanoma patients, and their potential role in shaping clinical outcomes. Being aware of the tricky yet still enigmatic role of pDCs in tumor control or progression, deciphering the features of heterogeneous circulating and tumor-infiltrating pDC subsets may brighten our understanding on how to overrule pDCs' hijacking by tumor cells to improve clinical success.

## RESULTS

### **P3-pDCs (CD80<sup>+</sup>PDL1<sup>-</sup>) accumulated within tumor of melanoma patients and negatively correlated with clinical outcomes**

In accordance with the described pDC subsets in the literature, we explored pDC diversity in the blood and tumor of melanoma patients as well as the blood of HDs using the markers CD80, PDL1, Axl, CD2 and LAG3. Analysis of flow cytometry labellings of CD45<sup>+</sup>Lin<sup>-</sup>HLA-DR<sup>+</sup>CD11c<sup>-</sup>BDCA4<sup>+</sup> cells with viSNE (visualisation of t-distributed stochastic

neighbour embedding) algorithm run with clustering based on CD80, PDL1, Axl, CD2 and LAG3 markers revealed that the only clusters to differentiate at basal state are the Axl<sup>+</sup> population (AS DCs) and CD2-expressing pDCs (Supplementary figure 1a). To precisely decipher pDC diversity, we measured Axl, CD2, LAG3 and TRAIL expression on pDCs from the different groups. CD2 or LAG-3 expression by pDCs was studied after the exclusion of Axl<sup>+</sup> cells (to eliminate any contamination by AS DCs) and we observed that the basal frequencies of CD2<sup>-</sup>, CD2<sup>low</sup> and CD2<sup>hi</sup> pDCs (Supplementary figure 1b) and LAG-3<sup>+</sup> pDCs (Supplementary figure 1c) remained unchanged in patients compared to controls. Furthermore, we observed a slight infiltration of AS DCs at the tumor site, even though proportions were lower than in patients and HDs' blood (Supplementary figure 1d). Also, for each group studied, AS DCs did not express CD80 or PDL1 (which located them in the P0-pDCs portion of the PDL1/CD80 gating dot plot; Supplementary figure 1e) and their expressions of CD2, LAG-3 and TRAIL in patients remained unchanged when compared to HD (data not shown). Strikingly, viSNE analyses of CD45<sup>+</sup>Lin<sup>-</sup>HLA-DR<sup>+</sup> cells revealed that, within steady-state pDCs, P3-pDCs were present in the blood and tumor of melanoma patients (Figure 1a). Analyses with the FlowSOM (clustering with self-organising maps) algorithm that allowed to subdivide Lin<sup>-</sup>HLA-DR<sup>+</sup> cells in our samples depending on the expression of CD11c, BDCA2, CD80 and PDL1 also differentiated a CD80<sup>+</sup>PDL1<sup>-</sup> cluster within the CD11c<sup>-</sup>BDCA2<sup>+</sup> metacluster that represented P3-pDCs (Figure 2a and b). To further specifically assess the presence of pDC subpopulations based on CD80/PDL1 markers as defined by Alculumbre *et al.*<sup>38</sup> in melanoma patients, we depicted human plasmacytoid dendritic cells (pDCs or P0-pDCs) within Lin<sup>-</sup>HLA-DR<sup>+</sup>CD11c<sup>-</sup> as BDCA2<sup>+</sup>CD80<sup>-</sup>PDL1<sup>-</sup> cells (Figure 1b). Among HLA-DR<sup>+</sup>BDCA2<sup>+</sup> cells, P1-, P2- and P3-pDCs were defined as CD80<sup>-</sup>PDL1<sup>+</sup>, CD80<sup>+</sup>PDL1<sup>+</sup> and CD80<sup>+</sup>PDL1<sup>-</sup> respectively. In basal conditions, we observed in the tumor infiltrates a reduced frequency of P1-pDCs, whereas P2-pDCs' frequency increased when compared to HD blood (Figure 1c). Notably, we also highlighted an increased frequency of circulating and tumor-infiltrating P3-pDCs in patients when compared to HD (Figure 1c), as well as an increased frequency of P3-pDCs in tumor infiltrate compared to blood in melanoma patients. Even though performed in a rather small cohort of patients, we found no difference of circulating pDC

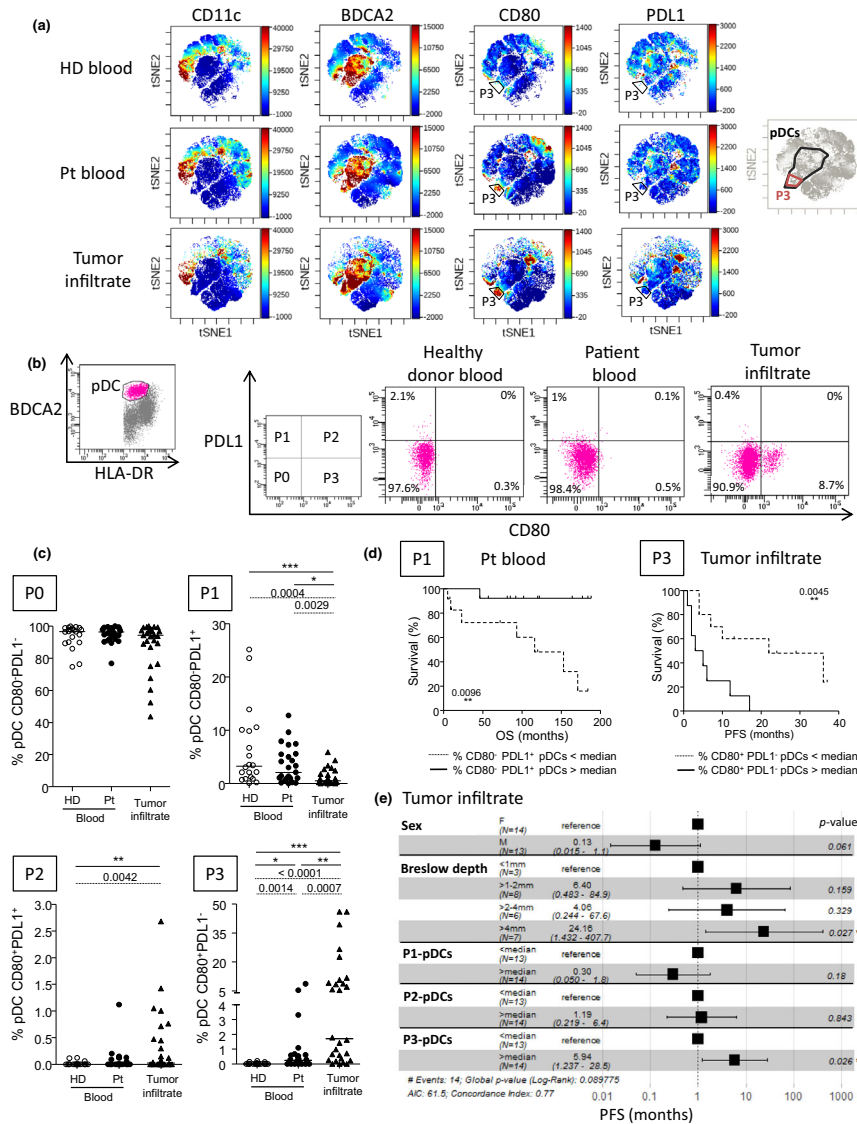


**Figure 1.** P3-(CD80<sup>+</sup>PDL1<sup>-</sup>)pDCs accumulate within the tumor and were linked to a bad clinical outcome. PBMC and tumor-infiltrating cells from melanoma patients together with PBMC from HD were labelled with specific antibodies allowing depicting the pDC subsets and submitted to flow cytometry analysis. **(a)** Concatenated tSNE plots showing CD11c, BDCA2, CD80 and PDL1 expression in CD45<sup>+</sup>Lin<sup>-</sup>HLA-DR<sup>+</sup>BDCA3<sup>-</sup> cells from HD blood (n = 20), Pt blood (n = 17) and tumor infiltrate (n = 27). Presented tSNE plots were based on proportional sampling and constructed after clustering with CD11c, BDCA2, BDCA1, CD80 and PDL1 markers by the viSNE algorithm (Cytobank). Black polygons encase P3-(CD80<sup>+</sup>PDL1<sup>-</sup>)pDCs seen only in melanoma patients. **(b)** Gating strategy for depicting P0-, P1-, P2- and P3-pDCs. After cell debris exclusion, single-cell gating and dead cell exclusion, CD45<sup>+</sup> cells were selected. Human plasmacytoid dendritic cells (pDCs or P0-pDCs) were then depicted as CD45<sup>+</sup>Lin<sup>-</sup>HLA-DR<sup>+</sup>CD11c<sup>-</sup>BDCA2<sup>+</sup> cells. CD80 and PDL1 allowed to further differentiate subpopulations amongst pDCs. P1-pDCs were defined as CD80<sup>-</sup>PDL1<sup>+</sup>, P2-pDCs as CD80<sup>+</sup>PDL1<sup>+</sup> and P3-pDCs as CD80<sup>+</sup>PDL1<sup>-</sup>. Representative flow cytometry dot plots displaying the frequencies of pDC subpopulations found on HD or patient blood and tumor infiltrate from melanoma patients. **(c)** Comparative frequencies of P0-, P1-, P2- and P3-pDCs within alive pDCs in the blood of healthy donors (HD, open circles, n = 20) or patients (Pt, filled circles, n = 25), and tumor infiltrate of melanoma patients (filled triangles, n = 28). Results are expressed as percentages of positive cells. One significant statistics are shown on the graphs. Bars indicate median. P-values were calculated using the Mann-Whitney (dashed lines) and Kruskal-Wallis (straight lines) non-parametric tests. \*P-value ≤ 0.05, \*\*P-value ≤ 0.01, \*\*\*P-value ≤ 0.001. **(d)** Comparative OS and PFS (from sampling time) of patients with low or high circulating P1-(left panel) or tumor-infiltrating P3-(right panel)pDCs. Groups were separated according to the median percentage of circulating P1-pDCs (2.1%, n = 12 or 13 patients/group) and tumor-infiltrating P3-pDCs (1.7%, n = 8 to 10 patients/group). Comparisons between groups were made using the Log-rank test. **(e)** Hazard ratios from comparative PFS (from sampling time) of gender, Breslow depth and frequencies of P1, P2- and P3-pDCs in the tumor infiltrate of melanoma patients (n = 27). For pDC frequencies, groups were separated using the median percentage of tumor-infiltrating P1-, P2- and P3-pDCs (0.50%, 0.04% and 1.7%, respectively). HD, healthy donor; Pt, patient.

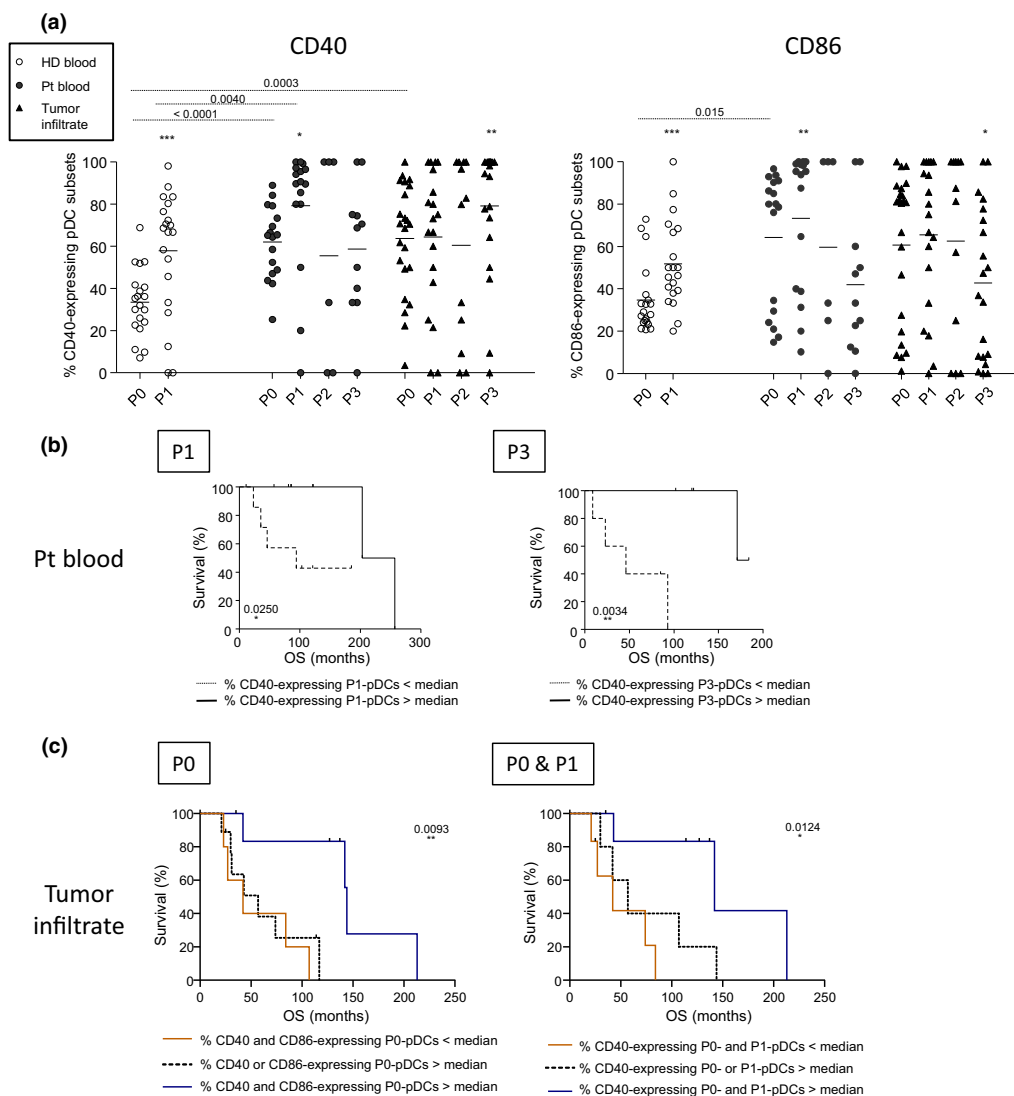


**Figure 2.** Circulating and tumor-infiltrating P0- and P1-pDCs displayed a higher basal activation status in melanoma patients and correlated with better OS. The basal expression of the co-activation molecules CD40 and CD86 on pDC subsets was analysed by flow cytometry within PBMCs and tumor-infiltrating cells of melanoma patients and HD, and their clinical relevance was assessed. **(a)** Expression levels of the co-stimulatory molecules CD40 and CD86 on P0-(CD80<sup>-</sup>PDL1<sup>-</sup>), P1-(CD80<sup>-</sup>PDL1<sup>+</sup>), P2-(CD80<sup>+</sup>PDL1<sup>+</sup>) and P3-(CD80<sup>+</sup>PDL1<sup>-</sup>)pDCs from the blood of healthy donors (HD, open circles,  $n = 20$ ) and melanoma patients (Pt, filled circles,  $n = 17$ ), and tumor infiltrates of melanoma patients (filled triangles,  $n = 23$ ). Results are expressed as percentages of positive cells within the corresponding pDC subpopulation (only samples displaying a proportion of pDC subset  $> 0\%$  are shown). Only significant statistics are shown on the graphs. Bars indicate mean.  $P$ -values were calculated using Mann-Whitney (dashed lines) and Wilcoxon signed rank (stars) non-parametric tests. Stars indicate significant differences compared to the P0 subset within each group. \* $P$ -value  $\leq 0.05$ , \*\* $P$ -value  $\leq 0.01$ , \*\*\* $P$ -value  $\leq 0.001$ . **(b)** Comparative OS (from diagnosis and sampling time; left and right panels respectively) of patients with low or high circulating CD40-expressing P1- or P3-pDCs. Groups were separated using the median percentage of circulating CD40-expressing P1 or P3 amongst the corresponding pDC subsets (90.24% and 68.75%, respectively,  $n = 5$  or 8 patients/group). **(c)** Comparative OS (from diagnosis time) of patients with low or high tumor-infiltrating CD40- and/or CD86-expressing P0-pDCs (left panel), and CD40-expressing P0- and/or P1-pDCs (right panel). Groups were separated using the median percentage of tumor-infiltrating CD40-expressing P0 (70.51%) and P1 (73.15%), and CD86-expressing P0 (80.68%) amongst the corresponding pDC subsets ( $n = 5$ –9 patients/group). **(b, c)** Comparisons between groups were made using the Log-rank test.

subsets' frequencies along melanoma progression (Supplementary figure 2c), and the three pDC subpopulations were found in the tumor of patients

independently of the tumor type (primary tumor, lymph node or cutaneous metastasis) (Supplementary figure 2d). To understand whether

the pattern of pDC subsets could distinguish patients from HD, we performed principal component analysis (PCA) (Figure 2e). Even though intragroups clustering by pDC subsets' frequency could not be achieved since each group was not located in distinct areas of the PCA (based on PC1 and PC2), the graph of variables illustrated that tumor infiltrates were mostly driven by P2- and P3-pDCs. We further deciphered CD2 and LAG-3 expression by circulating and tumor-infiltrating P0-, P1-, P2- and P3-pDCs that remained unchanged in patients when compared to controls (data not shown). Notably, the observed alterations of pDC subsets' frequencies seemed to associate with the clinical outcome of patients (Supplementary tables 3 and 4). Indeed, higher frequencies of circulating P1-pDCs were linked with better overall survival (OS), while high frequencies of tumor-infiltrating P3-pDCs negatively correlated with progression-free survival (PFS) (Figure 1d). Furthermore, we also examined the hazard ratios of pDC subpopulations combined with some major prognosticators of melanoma progression (such as Breslow depth and TNM classification). Patients who reported higher levels of circulating P1-pDCs were more likely to experience better clinical outcome, as indicated by their longer OS, than patients with low levels (HR = 0.068 and  $P$ -value = 0.029; Supplementary figure 2f). Strikingly, patients with higher levels of tumor-infiltrating P3-pDCs were six times more likely to undergo worse outcome, as indicated by shorter PFS than patients with low levels (HR = 5.94 and  $P$ -value = 0.026; Figure 1e). Thus, we unveiled for the first time an increased frequency of tumor-infiltrating P3-pDCs and an infiltration of AS DCs at the tumor site. Our data also pointed out that, in our small cohort of patients, P0-pDCs may potentially differentiate *in situ* into P3-pDCs that negatively correlated with melanoma patients' clinical outcomes.

### **Modulations of pDC subsets' basal activation status were observed in melanoma patients and differentially associated with clinical outcome**

To evaluate the basal activation status and cytotoxic capacity of pDC subpopulations in melanoma patients, we analysed the expression of co-stimulatory molecules (CD40, CD86) and TRAIL by P0-, P1-, P2- and P3-pDCs (Figure 2a, Supplementary figure 3a). We observed increased proportions and MFI of circulating and tumor-infiltrating CD40- and

CD86-expressing P0-pDCs in patients, together with an increased frequency or MFI of circulating and/or tumor infiltrating CD40-expressing P1-pDCs when compared to HD (Figure 2a, Supplementary figure 3a). In addition, within HD's and patient's blood groups, proportions and/or MFI of circulating and tumor-infiltrating CD40- and CD86-expressing P1-pDCs were higher than their P0-pDCs counterparts. Moreover, within patients' tumor infiltrates, there were higher proportions and MFI of CD40<sup>+</sup> P3-pDCs whereas lower frequencies of CD86<sup>+</sup> P3-pDCs when compared to P0-pDCs (Figure 2a, Supplementary figure 3a). Interestingly, we also observed higher MFI levels of CD40 and CD86 in tumor-infiltrating P3-pDCs than in patients' blood P3-pDCs (Supplementary figure 3a). Furthermore, regarding cytotoxic capacity, TRAIL basal expression by pDC subsets was left unchanged in melanoma patients when compared to controls (data not shown). Remarkably, the observed alterations of pDCs' basal activation status associated with the clinical outcome of patients (Supplementary tables 5 and 6). Higher proportions of circulating CD40<sup>+</sup> P1- and P3-pDCs predicted better clinical outcome (Figure 2b, Supplementary figure 3b). Strikingly, we also found that higher proportions of tumor-infiltrating CD40<sup>+</sup> CD86<sup>+</sup> P0-pDCs, and higher levels of both CD40-expressing P0- and P1-pDCs were associated with good outcome, as indicated by patients' longer OS (Figure 2c). Furthermore, we also examined the hazard ratios of CD40 and CD86 expression by pDC subpopulations. Patients who reported higher levels of both tumor-infiltrating CD40<sup>+</sup> P0- and P1-pDCs were more likely to undergo good clinical outcome, as indicated by longer OS than patients with low levels (HR = 0.27 and  $P$ -value = 0.047 for P0-pDCs and HR = 0.19 and  $P$ -value = 0.031 for P1-pDCs; Supplementary figure 3c). Altogether, these results highlighted that steady-state pDC subsets harboured a more activated status in the blood and tumor of melanoma patients compared to HDs, that overall correlated with a good clinical prognosis.

### **The diversification of pDCs into CD80/PDL1 subpopulations upon TLR7- and TLR9 triggering is perturbed in melanoma patients and correlated with clinical outcomes**

To investigate the diversification of circulating and tumor-infiltrating pDC subsets after TLR triggering, we monitored their frequency in

response to specific single or combined TLR ligands after 20 h of culture and assessed their clinical relevance (Figure 3, Supplementary figure 4a, Supplementary tables 3 and 4). After TLR7 or TLR9 stimulation (R848 and CpG<sub>A</sub> respectively), vi-SNE analyses showed that P1-, P2-, and P3-pDCs were found in HDs, patients' blood and tumor infiltrate (Figure 3a). Of note, P3-pDCs were visualised in tumor infiltrates without any TLR stimulation (condition "w/o stim"), which corroborated the observations of the basal status (Figure 1a–c). After 20 h culture in the absence of *ex vivo* stimulation by TLR-L (condition "stim –"), we observed less tumor-infiltrating P0-pDCs with a tendency towards the accumulation of P3-pDCs in patients when compared to controls, whereas we also found higher frequencies of circulating P1-pDCs in patients when compared to HDs (Figure 3b). After R848 or mix stimulation, the diversification of pDCs resulted in a decrease of the frequency of circulating P0-pDCs in HD and patients but such tendencies were observed to a lower extent for tumor-infiltrating P0-pDCs (not significant) (Figure 3b). Furthermore, within each group, we revealed increased proportions of P1- and P2-pDCs after 20 h-culture with TLR-L when compared to control conditions (the absence of stimulation) (Figure 3b). We also found higher frequencies of P1-pDCs in patients' blood after R848 or mix stimulation and lower proportions of P2-pDCs when compared to HDs' blood (Figure 3b). Yet, we observed lower levels of tumor-infiltrating P1- and P2-pDCs after R848 or mix stimulation when compared to HDs (Figure 3b). Interestingly, the higher frequencies of circulating P3-pDCs elicited in HD upon TLR triggering did not occur in patients' blood or tumors, probably given the pre-existing high levels of tumor-infiltrating P3-pDCs (Figure 3b). Intragroup clustering between patients' blood and tumor infiltrate was determined by PCA analysis, and frequencies of P3-pDCs with or without TLR stimulation seemed to differentiate the tumor infiltrate group from the others (Supplementary figure 4b). The heat map based on the frequencies of P0-, P1-, P2- and P3-pDCs in each sample type upon TLR stimulation illustrated the distinct patterns of pDC subpopulations' diversification in blood and tumor infiltrate of melanoma patients compared to HD (Supplementary figure 4c). After TLR triggering, we found lower frequencies of P1-pDCs at the tumor site than in blood, whereas an accumulation of tumor-infiltrating P3-pDCs

(Supplementary figure 4c). Interestingly in the absence of TLR triggering, higher frequencies of 20 h-cultured circulating P1-pDCs were linked to better OS (Supplementary figure 4d), while higher proportions of tumor-infiltrating P3-pDCs were linked to a worse clinical outcome (Supplementary figure 4e), as already witnessed at the basal state (Figure 1d). In addition after stimulation with the mixture of TLR-L, higher frequencies of tumor-infiltrating P0-pDCs were linked to a better OS (Supplementary figure 4e). Taken together, these results indicate that the diversification of circulating and tumor-infiltrating pDC subsets towards P1-, P2- and P3-pDCs prompted by TLR-L is perturbed in melanoma patients, with a failure to elicit P1- and/or P2-pDC subsets at the tumor site, and a preferential driving towards P3-pDCs which negatively correlated with clinical outcome.

#### **Tumor-infiltrating P1- (CD80<sup>-</sup>PDL1<sup>+</sup>) and P3-pDCs (CD80<sup>+</sup>PDL1<sup>-</sup>) displayed an altered capacity to further upregulate activation markers upon TLR triggering in melanoma patients**

To explore the functional capacity of circulating and tumor-infiltrating pDC subsets to respond to TLR triggering, we examined their expression of co-stimulatory molecules in response to specific single or combined TLR ligands after 20 h of culture (Figure 4, Supplementary figure 5). In the absence of *ex vivo* stimulation by TLR-L (condition "stim –"), frequencies of circulating and/or tumor-infiltrating CD40<sup>+</sup> P0-, P1- and P3-pDCs were more elevated in patients compared to HDs (Figure 4a, Supplementary figure 5), revealing a higher ability of pDCs' subpopulations to partially mature *in situ* in melanoma patients. After TLR stimulation, the proportions of CD40-expressing P1- and P3-pDCs increased in HD blood when compared to unstimulated conditions, while levels remained high in patients independently of TLR triggering, suggesting that these cells already reached a certain level of activation *in situ* (Figure 4a). Furthermore, frequencies of CD86-expressing P1- and P3-pDCs increased in HD blood after R848 or/and mix stimulation and, even though such tendencies were found in patient's blood, they were not observed in tumor-infiltrating P1- and P3-pDCs (Figure 4a). Moreover, levels of tumor-infiltrating CD86<sup>+</sup> P3-pDCs after R848 and mix stimulation were significantly lower in patients when compared to HD blood (Figure 4a). In

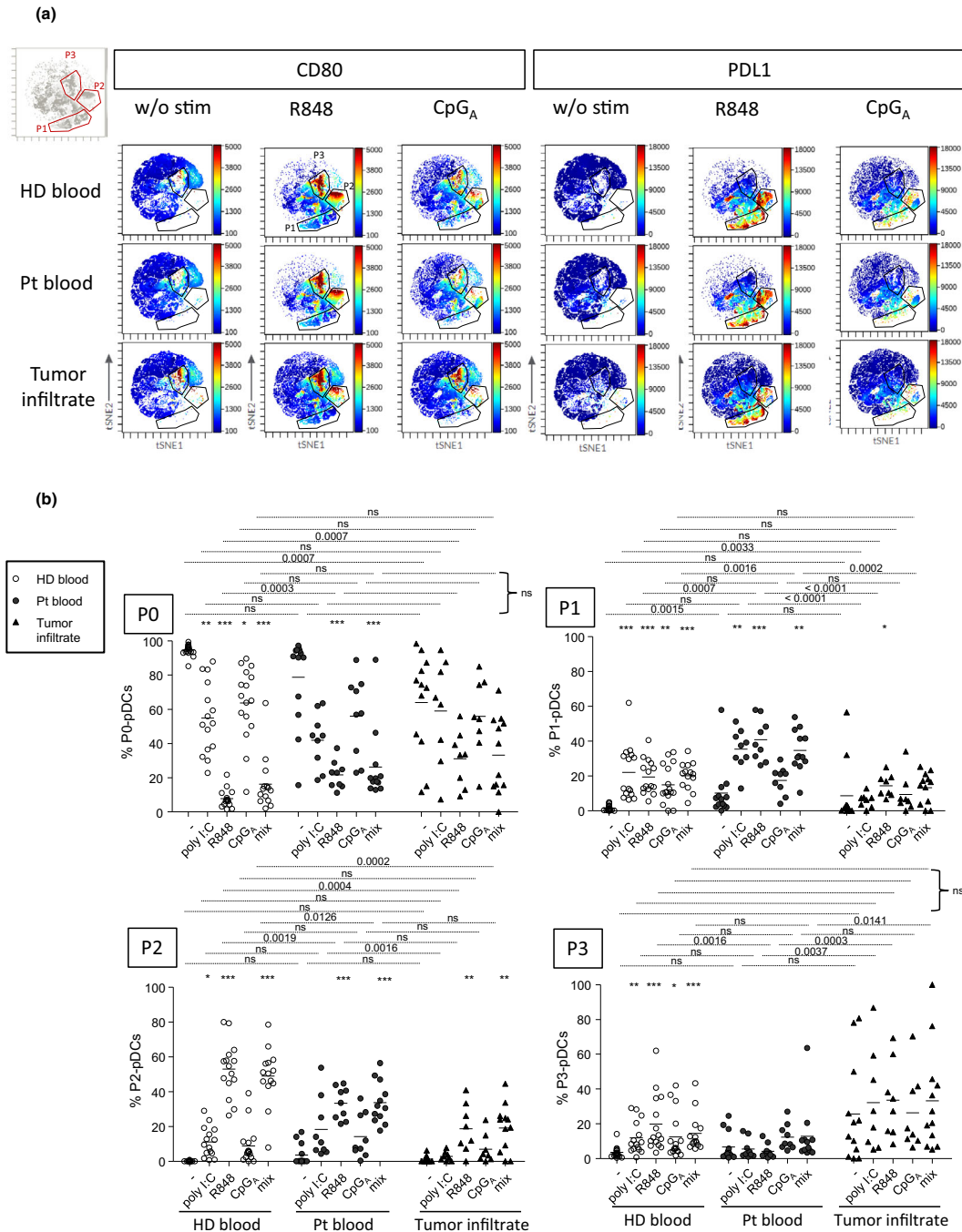


**Figure 3.** The diversification of P0-pDCs into CD80/PDL1 subpopulations upon TLR-7 or TLR-9 stimulation was altered in the blood and tumor of melanoma patients. Cell suspensions from blood (HD, *n* = 18; Pt, *n* = 13) or tumor infiltrates (Pt, *n* = 12) were stimulated or not for 20 h with or without TLR ligands (poly:I:C, R848 or CpG<sub>A</sub>) alone or mixed together (mix), and the proportions of the different pDC subpopulations (P0, P1, P2, P3) were assessed using flow cytometry. **(a)** Concatenated tSNE plots showing CD80 and PDL1 expression in CD45<sup>+</sup>HLA-DR<sup>+</sup>BDCA4<sup>+</sup> cells from HD blood (*n* = 7), Pt blood (*n* = 6), and tumor infiltrate (*n* = 5) with (R848, CpG<sub>A</sub>) or without (w/o stim) TLR stimulation. Presented tSNE plots are based on proportional sampling and constructed after clustering with AxL, CD80 and PDL1 markers by the viSNE algorithm (CytoBank). Black polygons encase P1-(CD80<sup>+</sup>PDL1<sup>+</sup>), P2-(CD80<sup>+</sup>PDL1<sup>-</sup>) and P3-(CD80<sup>-</sup>PDL1<sup>-</sup>) pDCs seen after TLR stimulation. **(b)** Comparative frequencies of P0-, P1-, P2- and P3-pDCs within alive pDCs in the blood of healthy donors (HD, open circles, *n* = 18), patients (Pt, filled circles, *n* = 13), and tumor infiltrate of melanoma patients (filled triangles, *n* = 12). Results are expressed as percentages of positive cells within pDCs. Bars indicate mean. Stars indicate significant differences compared to the control condition without stimulation (-) within each group. *P*-values were calculated using Mann-Whitney (dashed lines) and Kruskal-Wallis (stars) non-parametric tests. \**P*-value ≤ 0.05, \*\**P*-value ≤ 0.01, \*\*\**P*-value ≤ 0.001.

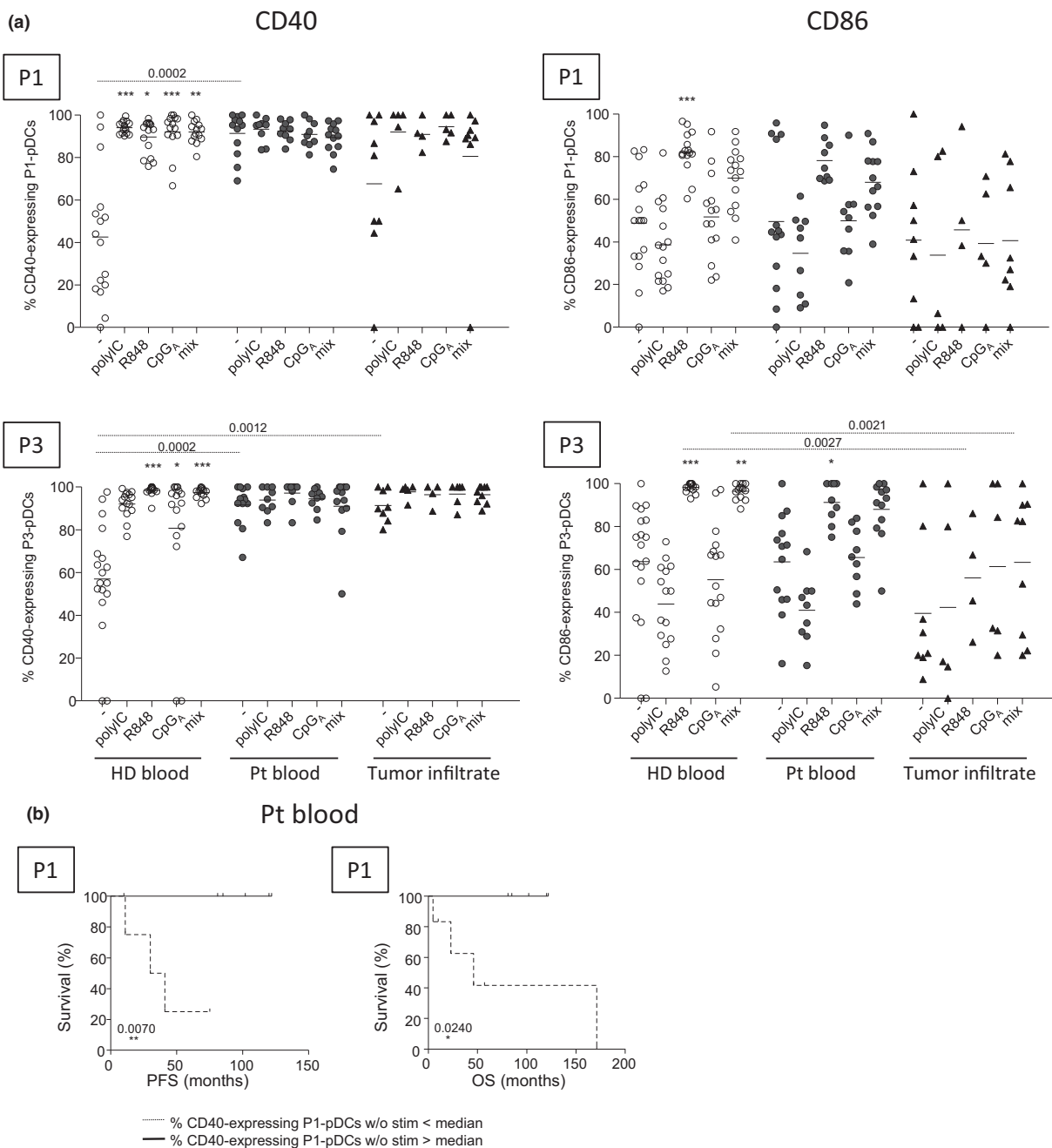


**Figure 4.** Variations of co-stimulatory molecule expression on pDC subsets in melanoma patients after *ex vivo* TLR triggering. Cell suspensions from blood (HD,  $n = 18$ ; Pt,  $n = 13$ ) or tumor infiltrates (Pt,  $n = 10$ ) were stimulated or not for 20 h with or without TLR ligands (poly:I:C, R848 or CpG<sub>A</sub>) alone or mixed together (mix). The expression of the co-stimulatory molecules CD40 and CD86 were measured on P1- and P3-pDCs using flow cytometry and their clinical relevance was assessed. **(a)** Expression levels of the co-stimulatory molecules CD40 and CD86 on P1- (CD80<sup>+</sup>PDL1<sup>+</sup>) and P3-(CD80<sup>+</sup>PDL1<sup>-</sup>)pDCs from the blood of healthy donors (HD, open circles,  $n = 18$ ) and melanoma patients (Pt, filled circles,  $n = 13$ ), and tumor infiltrates of melanoma patients (filled triangles,  $n = 10$ ). Results are expressed as percentages of positive cells within the corresponding pDC subpopulation (only samples displaying a proportion of pDC subset > 0% are shown). Only significant statistics are shown on the graphs. Bars indicate mean. Stars indicate significant differences compared to the control condition without stimulation (-) within each group. *P*-values were calculated using Mann-Whitney (dashed lines) and Kruskal-Wallis (stars) non-parametric tests. \**P*-value  $\leq 0.05$ , \*\**P*-value  $\leq 0.01$ , \*\*\**P*-value  $\leq 0.001$ . **(b)** Comparative PFS and OS (from sampling time) of patients with low or high circulating CD40-expressing P1-pDCs without *ex vivo* TLR stimulation. Groups were separated using the median percentage of circulating CD40-expressing P1 (CD80<sup>+</sup>PDL1<sup>+</sup>) amongst pDCs without TLR triggering (95.3%,  $n = 5-7$  patients/group). Comparisons between groups were made using the Log-rank test.

addition, proportions of circulating CD40-expressing P0-pDCs after mix stimulation increased in HDs, whereas decreased in patients when compared to controls (Supplementary figure 5). Regarding P2-pDCs, in the absence of TLR stimulation, we observed a tendency for lower proportions of tumor-infiltrating CD86<sup>+</sup> cells when compared to HDs (Supplementary figure 5). Also, TLR stimulation (polyI:C and CpG<sub>A</sub>) triggered a drop of the frequency of CD86<sup>+</sup> P2-pDCs in HDs that was not significant in patients (although tendencies were seen in patients' blood) and no differences were found in the frequencies of CD40<sup>+</sup> P2-pDCs between patients and controls (Supplementary figure 5). To assess the clinical relevance of our findings, we performed correlations between 20 h-cultured circulating or tumor-infiltrating pDC features (activation status upon TLR-L stimulation) and clinical outcomes (Supplementary tables 5 and 6). In the absence of *ex vivo* stimulation by TLR-L, higher proportions of circulating CD40-expressing P1-pDCs were associated with a better clinical outcome as they were linked to longer PFS and OS (Figure 4b). Alterations of the frequencies of CD40- and CD86-expressing pDC subsets after TLR stimulation in patients did not affect clinical outcome. Thus, tumor-infiltrating P1- and P3-pDCs from melanoma patients displayed an altered capacity to further upregulate co-stimulatory molecules upon TLR7-/9- stimulation, yet the activation status of circulating P1-pDCs triggered *in situ* was correlated to clinical outcome.

### The functionality of pDC subsets upon TLR triggering is altered in the context of melanoma

We further investigated the functional properties of circulating and tumor-infiltrating pDC subsets by assessing their ability to produce cytokines and chemokines and exhibit cytotoxicity upon TLR triggering. We performed intracellular labelling of IFN $\alpha$ , IP-10, and IL6, and measured surface TRAIL expression within CD80/PDL1 pDC subsets stimulated or not with TLR-Ls (Figure 5a, Supplementary figures 6–8). We first defined the optimal kinetic of TLR stimulation allowing to obtain both the differentiation of CD80/PDL1 pDC subsets and the production of intracellular cytokines and chemokines (Supplementary figure 6). By comparing the frequency of HDs' pDC subsets and their expression of the different

parameters analysed upon TLR triggering at different time points (5h, 8h, 18h and 24h), we estimated that pDCs (P0-pDCs) optimally differentiated into the distinct pDC subsets (P1-, P2- and P3-pDCs) (Supplementary figure 6a), expressed TRAIL (Supplementary figure 6b), and produced the analysed cytokines and chemokines after 18h of culture (even though the assessment of IFN $\alpha$  and IP-10 production was not optimal after R848 stimulation at this time point; Supplementary figure 6c). We therefore used this time point to assess the functionality of pDC subsets in melanoma patients. In the absence of *ex vivo* stimulation by TLR-L (condition w/o stim), we observed lower frequencies of circulating and/or tumor-infiltrating IL6<sup>+</sup> P3-pDCs and TRAIL<sup>+</sup> P1-pDCs in patients when compared to HD (Figure 5a and b). While upon TLR stimulation circulating P1- and P3-pDCs from patients were able to secrete IFN $\alpha$  and/or express TRAIL, they had an impaired production of IP-10 when compared to HDs (Figure 5a and b). Interestingly, the functionality of tumor-infiltrating P1- and P3-pDCs after TLR triggering was totally abrogated. Since P1-pDCs are known for their capacity to produce IFN $\alpha$  after TLR triggering, we performed Spearman correlations between proportions of P1-pDC and frequencies of IFN $\alpha$ <sup>+</sup> pDCs upon TLR triggering in the corresponding samples (Supplementary table 7, Figure 5c). Significant positive correlations were found between circulating or tumor-infiltrating P1-pDCs and IFN $\alpha$ -producing pDCs after mix or CpG<sub>A</sub> stimulation, respectively (Figure 5c). In addition, in tumor infiltrates after 20 h culture without *ex vivo* TLR stimulation, Spearman correlations performed between P1- and P2-pDC subsets' proportions within CD45<sup>+</sup> cells and levels of TGF $\beta$  secretion revealed significant negative correlations between these two parameters (Supplementary table 8, Figure 5d). Furthermore, we observed that after TLR triggering, circulating and tumor-infiltrating P0-pDCs were capable to produce IFN $\alpha$ . While circulating P2-pDCs could produce IP-10 as HDs upon CpG<sub>A</sub> stimulation, tumor-infiltrating P2-pDCs were defective for this function (Supplementary figure 7a). Interestingly, circulating and tumor-infiltrating P0-pDCs from patients were unable to upregulate TRAIL in response to R848 triggering (Supplementary figure 7b). Analyses with the FlowSOM algorithm allowed to perform a comparative overview of pDC subsets' functionality, and to visualise as well as quantify potential differences between groups by analysing

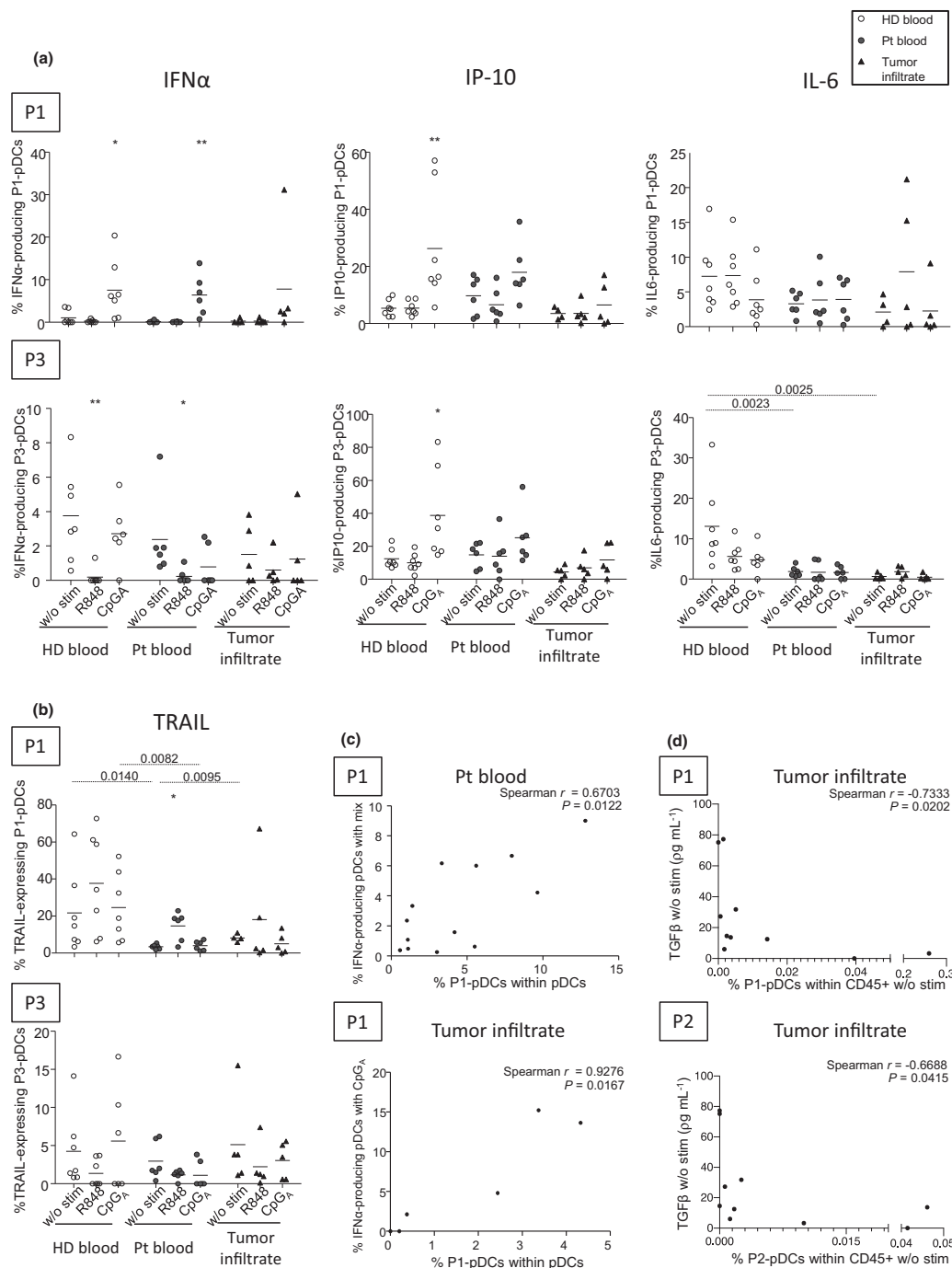


**Figure 5.** Altered functionality of circulating and tumor-infiltrating P1- and P3-pDCs correlated with IFN $\alpha$  and TGF $\beta$  levels within tumor infiltrates in melanoma patients. Cell suspensions from blood (HD,  $n = 7$ , open circles; Pt,  $n = 6$ , filled circles) or tumor infiltrates (Pt,  $n = 5$ , filled triangles) were stimulated for 18h with or without TLR-L (R848 or CpG<sub>A</sub>) and (a) IFN $\alpha$  (left panels), IP10 (middle panels) and IL-6 (right panels) production and (b) TRAIL expression by P1- and P3-pDCs were evaluated using flow cytometry. Results are expressed as percentages of positive cells within the corresponding pDC subpopulation. Bars indicate mean. Stars indicate significant difference with control without stimulation within each group. Only significant statistics are shown on the graphs.  $P$ -values were calculated using Mann-Whitney (dashed lines) and Kruskal-Wallis (stars) non-parametric tests. \* $P$ -value  $\leq 0.05$ , \*\* $P$ -value  $\leq 0.01$ , \*\*\* $P$ -value  $\leq 0.001$ . (c) Spearman's correlations of IFN $\alpha$ -producing pDCs after TLR-L stimulation (mix or CpG<sub>A</sub>) with the proportion of circulating ( $n = 13$ ) and tumor-infiltrating ( $n = 6$ ) P1-pDCs, respectively, in the corresponding samples. (d) Spearman's correlations upon culture without TLR-L stimulation of TGF $\beta$  secretion by whole tumor-infiltrating cells with proportions of tumor-infiltrating P1- and P2-pDCs within CD45<sup>+</sup> cells ( $n = 10$ ).

the transformed MFI of each marker (IFN $\alpha$ , IP-10 and TRAIL; Figure 6). These analyses allowed clusterisation of "pure" pDCs (Lin<sup>-</sup>HLA-DR<sup>+</sup>CD11c<sup>-</sup>BDCA2<sup>+</sup>Axl<sup>-</sup> cells) in the samples depending on the expression of CD80 and PDL1. We obtained several metaclusters corresponding to pDC subpopulations (Figure 6a). Upon quantification of the cytokine levels for each metacluster, we confirmed a decreased IP-10 production by tumor-infiltrating P1-, P2- and P3-pDCs after CpG<sub>A</sub> or R848 respectively, while tumor-infiltrating P1-pDCs expressed significantly less TRAIL than circulating cells from patients and HDs (Figure 6b). In addition, circulating P3-pDCs from patients expressed lower levels of IFN $\alpha$  when compared to HDs. IL-6 production was also decreased in patients by circulating P0- and P3-pDCs after TLR stimulation when compared to controls (Supplementary figure 7c). Such analysis revealed a perturbed functionality of pDC subsets in melanoma patients. To propose a fully comprehensive analysis, we also decipher the functionality of the previously identified pDC subsets based on CD2 or LAG3 markers as well as AS-DCs. Regarding the CD2-expressing pDCs (CD2<sup>low</sup>, CD2<sup>hi</sup>), we depicted them after excluding Axl<sup>+</sup> cells from the analysis. However, given the low levels of CD2<sup>hi</sup>Axl<sup>-</sup> pDCs in the three groups (Supplementary figure 1b), only observations on CD2<sup>low</sup> pDCs will be discussed. Upon TLR stimulation, IFN $\alpha$  production and/or TRAIL expression were triggered in circulating CD2<sup>-</sup> and CD2<sup>low</sup> pDCs from patients as in HDs, and this was also the case for circulating IP-10-expressing CD2<sup>low</sup> pDCs (Supplementary figure 8a). Interestingly, we observed a defective ability of tumor-infiltrating CD2<sup>-</sup> and CD2<sup>low</sup> pDCs to express IP-10 and upregulate TRAIL compared to HD (Supplementary figure 8a). Regarding LAG-3<sup>+</sup> pDCs, higher frequencies of circulating IP-10-expressing cells were observed in patients' blood upon CpG<sub>A</sub> stimulation when compared to HD, while the production of IFN $\alpha$ , IL6, and TRAIL remained unchanged (with or without TLR stimulation) (data not shown). Concerning AS DCs, high frequencies of TRAIL-expressing cells upon TLR triggering found in HDs were abrogated in patients (Supplementary figure 8b). Taken together, even though performed in a rather small cohort of patients, our findings highlighted differential alterations of the functional response (cytotoxicity and cytokine production) of pDC subsets and AS

DCs following TLR triggering in melanoma patients when compared to HDs.

## DISCUSSION

pDCs play a critical yet enigmatic role in antitumor immunity. Despite proof of pDC diversity in physiological, autoimmune, infectious or malignant conditions, pDCs have been studied as a whole population so far in cancer, and the assessment of individual pDC subsets is needed to fully grasp their involvement in cancer immunity. In this study, we provide an integrated overview of the phenotypic and functional features of several circulating and tumor-infiltrating pDC subsets (based on CD80/PDL1, CD2 or LAG3 markers) in melanoma patients together with their link with clinical outcome (Figure 7). Such understanding reveals the potential involvement of pDC subpopulations in shaping clinical outcomes. Our study shed light for the first time on the phenotypic heterogeneity of pDCs in melanoma. Thus, pDC diversity should be considered for the development of novel therapeutic strategies by targeting a specific pDC subset in order to optimise antitumor immunity and achieve better clinical success.

Our work represents the first study depicting simultaneously the phenotypic and functional features of several pDC subsets both in circulation and within tumor microenvironment in the context of cancer, and to assess their correlation with clinical outcome. Recent reports using single-cell RNA-seq and high-dimensional phenotypic mapping highlighted diversity in DC compartments,<sup>32,33</sup> especially the existence of phenotypically distinct human blood pDC subsets.<sup>32,33,38</sup> By exploring such pDC subsets using multiparametric flow cytometry, we revealed the coexistence of distinct pDC subsets and precursor DCs (AS DCs) in melanoma tumors. We observed an increased frequency of P3-pDCs (CD80<sup>+</sup>PDL1<sup>-</sup>) in the blood of melanoma patients compared to HD, together with their accumulation within the tumor, which was linked to a bad clinical outcome. Consistently, we previously underlined in two independent cohorts of melanoma patients that the accumulation of pDCs within the tumor was linked to a bad clinical outcome,<sup>15</sup> and that high frequencies of tumor-infiltrating CD80-expressing pDCs were linked with a bad prognosis.<sup>40</sup> Thus, compiled with recent findings,

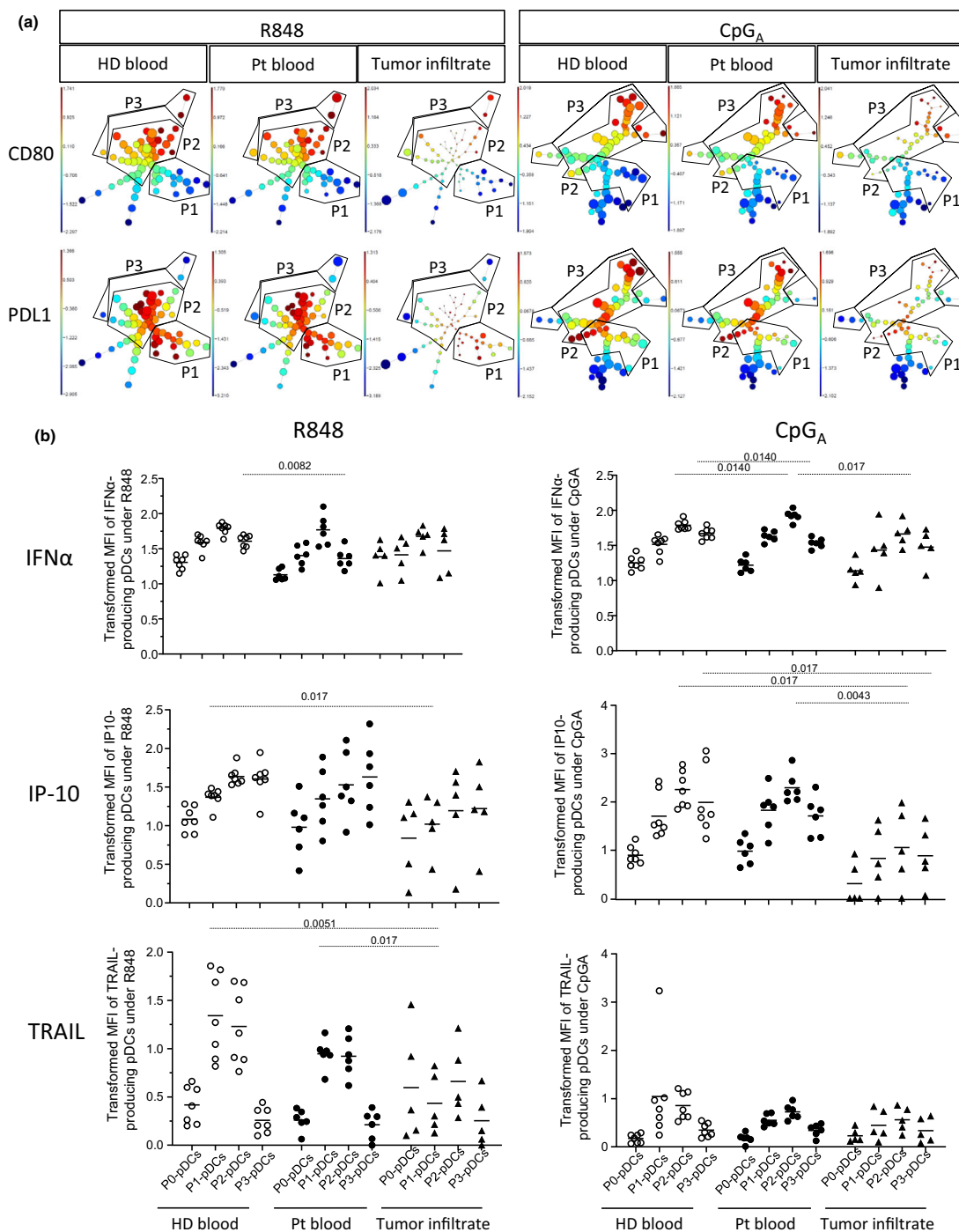


**Figure 6.** P1-pDCs from melanoma patients exhibited alterations of IFN $\alpha$ , IP10 and TRAIL expression when compared to healthy donors. **(a)** Aggregated minimum spanning trees (MSTs) of CD45<sup>+</sup>HLA-DR<sup>+</sup>BDC4<sup>+</sup>Axl<sup>-</sup> cells from HD blood ( $n = 7$ ), Pt blood ( $n = 6$ ) and tumor infiltrate ( $n = 5$ ) samples following 18h culture with R848 (left panels) or CpG<sub>A</sub> (right panels). MSTs are colored by CD80 and PDL1 expression and were derived from FlowSOM analyses (Cytobank) performed on viSNE analyses constructed after clustering of CD45<sup>+</sup>HLA-DR<sup>+</sup>BDC4<sup>+</sup>Axl<sup>-</sup> cells with CD80 and PDL1 markers. Black polygons encase P1-(CD80<sup>+</sup>PDL1<sup>+</sup>), P2-(CD80<sup>+</sup>PDL1<sup>+</sup>) and P3-(CD80<sup>+</sup>PDL1<sup>-</sup>)pDCs seen after R848 (left panels) or CpG<sub>A</sub> (right panels) stimulation. **(b)** Transformed MFI of IFN $\alpha$ , IP10 and TRAIL respectively on IFN $\alpha$ -, IP10- and TRAIL-producing pDC subsets from HD blood ( $n = 7$ ), Pt blood ( $n = 6$ ) and tumor infiltrate ( $n = 5$ ) samples following 18h culture with R848 (right panels) or CpG<sub>A</sub>. Raw data (MFI) were derived from FlowSOM analyses (Cytobank) and transformed using the hyperbolic arcsinh function. Only significant statistics are shown on the graphs.

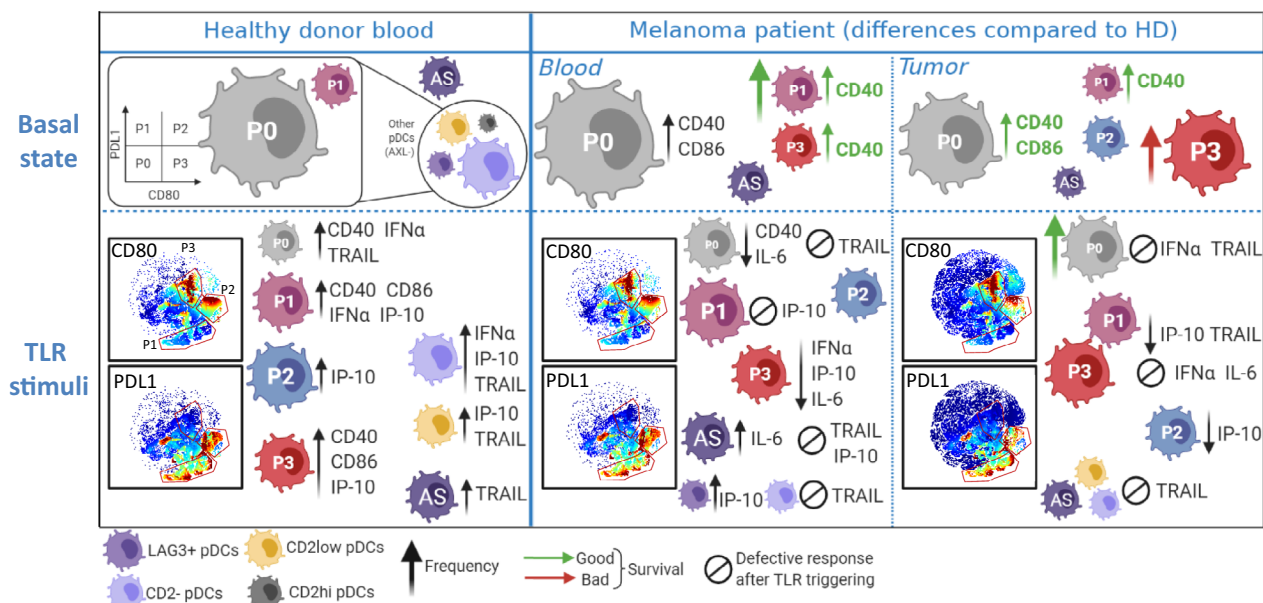


**Figure 7.** Overview of the diversity of circulating and tumor-infiltrating pDC subsets in melanoma patients and their relation to clinical outcomes. pDCs’ diversity was monitored based on CD80/PDL1 expression, as well as CD2, LAG3 and Axl markers. By assessing the frequency, the basal activation level, the diversification and functionality upon TLR triggering, we highlighted that specific circulating and tumor-infiltrating pDC subsets correlated with clinical outcomes in melanoma patients. At basal state (upper part of the figure), we observed a decrease in P1-pDCs along with an increase in P2- and P3-pDCs in the blood and tumor infiltrate of melanoma patients compared to healthy donors’ blood. Accumulation of P3-pDCs within the tumor drove a poor clinical outcome, whereas activated P0- and P1-pDCs were associated with better survival. TLR triggering (lower part of the figure) prompted the diversification towards P1-, P2- and P3-pDCs in healthy donors, which were able to upregulate costimulatory molecules (CD40, CD86), to secrete IFN $\alpha$ , IP10, and to exhibit TRAIL expression. In both blood and tumor of melanoma patients, we underlined a deficient diversification of pDCs, which were strongly impaired in their functionality.

our data suggests that P0-pDCs (CD80<sup>-</sup>PDL1<sup>-</sup>) preferentially differentiate *in situ* in tumors into P3-pDCs which negatively associated with clinical outcome in melanoma patients. Furthermore, we previously demonstrated that pDCs’ hijacking by tumor cells induced pro-tumoral regulatory and Th2 immune responses through OX40L and ICOSL,<sup>16</sup> and impacted pDCs’ cross-talk with antitumor immune effectors<sup>15</sup> (NK, T cells and  $\gamma\delta$  T cells).<sup>41</sup> Notably, in the initial discovery by Alculumbre *et al.*, whereas P1-pDCs were specialised in type I IFN production, P3-pDCs were shown to promote T-cell activation and Th2 differentiation and upregulate OX40L and CD40/CD86 activation markers.<sup>38</sup> Notably, the transcriptomic signature of P3-pDCs revealed CCL22 (MDC) as highly produced by this subset,<sup>38</sup> indicating that P3-pDCs may preferentially attract CCR4<sup>+</sup> Th2 and regulatory T cells.<sup>42,43</sup> It will be very interesting to further decipher in melanoma the role of each pDC subset in subsequently triggering specific Th profiles and orienting antitumor immunity.

The mechanisms by which melanoma drives the differentiation of P3-pDCs remains to be elucidated. In healthy conditions, pDC diversification into the three phenotypically and functionally distinct subpopulations occurred within 8 to 24h after a single TLR7 (Flu) or TLR-9 (CpGA, CpGB) stimulus,<sup>38</sup> and a TNF-mediated autoregulatory loop was the main factor controlling P3 differentiation.<sup>38</sup> Recently, HDs’ P0-pDCs were shown to properly differentiate into functional P1-, P2- and P3-pDCs upon 24 h culture with SARS-CoV-2.<sup>39</sup> Interestingly, hydroxychloroquine inhibited pDC diversification, especially P2-/P3-pDC subsets, suggesting a role for endosomal acidification in this process. In autoimmune context, the accumulation of the P1-pDCs population in both blood and skin of patients with lupus or psoriasis revealed to be driven by LL37-DNA complexes.<sup>38</sup> In the absence of *ex vivo* stimulation by TLR-L in HDs, we witnessed a basal level of intracellular cytokine production in circulating P1-, P2- and P3-pDCs (unseen in P0-pDCs) suggesting a natural *in vivo* pDC activation upon pDC diversification. Furthermore, in patients we also

observed a weak production of IFN $\alpha$ , IP-10 and IL-6 by circulating and tumor-infiltrating pDC subsets especially P2-pDCs, suggesting an *in situ* activation of these cells. *In situ* diversification of pDCs in melanoma could be driven by damage-associated molecular patterns (DAMPs) released by tumor cells following immunogenic cell death,<sup>44</sup> activation of the cGAS-cGAMP-STING pathway by cytosolic DNA,<sup>45</sup> complexes of self-DNA/RNA with cathelicidin (LL37)<sup>46,47</sup> or mitochondrial DNA,<sup>48</sup> or from soluble factors released by tumors cells such as alarmin IL-33 which was shown to affect DC maturation.<sup>49</sup> Such DC-activating signals remained to be identified in melanoma.

Regarding functionality, in healthy context, P1-pDCs were shown to trigger mostly innate immunity (type I IFN), whereas P3-pDCs preferentially promoted adaptive immunity through T-cell activation.<sup>38</sup> Indeed, P1-pDCs produced high levels of type I IFN, IL6, IL8, and P3-pDCs mostly expressed costimulatory molecules (CD40, CD86) and ICOSL. In the present study, we uncovered a perturbed functionality of pDC subsets in both blood and tumors of melanoma patients. Tumor-infiltrating P1- and P3-pDCs from melanoma patients displayed an altered capacity to further upregulate co-stimulatory molecules upon TLR7/9 stimulation. Furthermore, while circulating P1- and P3-pDCs from patients were able to secrete IFN $\alpha$  and/or express TRAIL upon TLR stimulation, they had an impaired production of IP-10 when compared to HDs. Interestingly, tumor-infiltrating P1-, P2- and P3-pDCs were defective in producing IP-10 upon CpG<sub>A</sub> or R848 respectively, while tumor-infiltrating P0- and P1-pDCs from patients seemed to be unable to upregulate TRAIL in response to R848 triggering. Such observations suggest that P1-pDCs may exhibit a less direct TRAIL-mediated cytotoxic potential towards tumor cells.<sup>50,51</sup> In addition, the proportion of tumor-infiltrating P1-pDCs was positively correlated with IFN $\alpha$ -producing pDCs after TLR-L stimulation, but negatively correlated with levels of TGF $\beta$ . Altogether, our study, even though performed in a rather small cohort of patients, highlighted defective innate immune functions of pDC subsets in melanoma while accumulation of P3-pDCs that may favor Treg/Th2 cell recruitment.

Previous studies demonstrated that CD2 expression could distinguish two pDC subsets in the blood of HD: CD2<sup>hi</sup> and CD2<sup>low</sup> pDCs. Both

subsets produce IFN $\alpha$ , TNF $\alpha$ , IL6 and express granzyme B and TRAIL, but CD2<sup>hi</sup> pDCs uniquely express lysozyme and secrete higher levels of IL12p40,<sup>26</sup> and display more efficiency in triggering proliferation of naïve allogeneic T cells, and a survival advantage during stress and upon exposure to glucocorticoids.<sup>27</sup> Within CD2<sup>hi</sup> pDCs, a scarcer CD2<sup>hi</sup>CD5<sup>+</sup>CD81<sup>+</sup> pDC subset was also described in blood, bone marrow and tonsils.<sup>28</sup> After TLR stimulation, they produced very little type I IFN but high IL12p40, IL6, IL8 and were potent stimulators of B-cell activation and strong inducers of T-cell proliferation and regulatory T cells. However, these studies did not exclude AS DCs from the analyses, thus CD2<sup>hi</sup> pDCs could actually be AS DCs. After exclusion of Axl<sup>+</sup> cells, we found an Axl<sup>-</sup>CD2<sup>hi</sup> pDC population which represented < 3% amongst pDCs in steady state or after TLR triggering in the three studied groups, rendering further studies of these cells challenging. Yet, we studied Axl<sup>-</sup>CD2<sup>low</sup> pDCs which were similarly represented in melanoma patients compared to HD (70–80% of pDCs being CD2 negative). Also, P0- and P1-pDCs expressed similar levels of CD2 between the groups. Interestingly, about 40–50% of P1-pDCs expressed CD2, whereas only 30% of P0-pDCs were positive for this marker. However, upon TLR stimulation, we observed a defective ability of tumor-infiltrating CD2<sup>-</sup> and CD2<sup>low</sup> pDCs to express CXCL10 and upregulate TRAIL compared to HD. Thus, melanoma did not seem to specifically modulate CD2-expressing pDCs. Interestingly, CD2<sup>low</sup> pDCs were shown to be depleted in HIV patients,<sup>37</sup> suggesting that HIV may influence the trafficking of pDC subsets, their survival or potential interconversion between the subsets.

LAG3 has also been proposed as a candidate to define pDC subsets. Indeed, LAG3<sup>+</sup> pDCs (representing 6% of total circulating pDCs), were found to be enriched at the tumor site of melanoma patients endowed with a partially activated phenotype.<sup>13</sup> LAG3 interaction with CMH-II induced a TLR-independent activation of pDCs with limited IFN $\alpha$  but high IL6 production. LAG3<sup>+</sup> pDCs were shown to express higher levels of CD80, CD86 and TRAIL than LAG3<sup>-</sup> pDCs, and to drive an immune-suppressive environment.<sup>13</sup> In our study, we observed no differences between the groups regarding the proportion of LAG3 pDCs, but our small cohorts would need to be complemented by larger studies.

Whereas the production of IFN $\alpha$ , IL6 and expression of TRAIL upon TLR stimulation were similar, we noticed an increased production of CXCL10 by circulating LAG3<sup>+</sup> pDCs from melanoma patients after CpG<sub>A</sub> stimulation. Further analyses will be required on large cohorts to assess the potential connectivity between P1- or P3-pDCs and LAG3<sup>+</sup> pDCs.

The population of AS DCs features an intermediate status between pDCs and cDCs.<sup>6,32,33</sup> As a result of their expression of BDCA2, CD123, these cells were often wrongly taken when analysing pDCs, but should be considered as an independent precursor DC subset identifiable through Axl expression. In our study, AS DCs clearly segregated into an independent cluster. We observed a slight infiltration by AS DCs at the tumor site, even though proportions were lower than in patients and HDs' blood. In addition, while AS DCs from HD exhibited TRAIL upon TLR triggering, such functionality was down-modulated or abrogated in circulating and tumor-infiltrating AS DCs from patients. Such observations suggested that melanoma can recruit these DC precursors while subverting their functions early on. Besides, AS DCs (Axl<sup>+</sup>Siglec6<sup>+</sup>) were found to infiltrate human skin during wounding.<sup>36</sup>

Our present work together with previous studies highlights that the diversity of pDCs' effects in many physiological and pathological conditions may be mediated by distinct pDC subsets differing in phenotype and function. It has been demonstrated in mice that type I IFN response upon pathogens encounter and antitumor immunity were attributable to CD9<sup>+</sup> SiglecH<sup>low</sup> pDCs, whereas CD9<sup>-</sup> SiglecH<sup>hi</sup> pDCs promoted tolerance and were found to accumulate within tumors.<sup>31</sup> Recently, a newly described BDCA2<sup>+</sup> CD123<sup>int</sup> CD1a<sup>+</sup> pDC subset was shown to rapidly infiltrate human skin during wounding.<sup>36</sup> Thus, depending on the nature of the environmental stimuli, pDCs may diversify in specific cell fate in order to optimally adjust to the danger to face.

Our results, based on a still limited cohort of patients, represent preliminary findings for an extended study. Yet, our study highlights distinct specialised pDC subsets, which might be subverted in pathologic situations, but could be therapeutically exploited to trigger protective immune responses in cancers, infections, and autoimmune diseases. Such novelty highlights the importance of considering pDC diversity when developing pDC-based therapeutic strategies to

ensure optimal clinical success. Such new level of pDC plasticity prompts the further deciphering of pDC complexity to better understand and exploit these potent immune players.

## METHODS

### Melanoma patients and HD samples

The study was conducted in accordance with the principles expressed in the Declaration of Helsinki. All procedures were approved by the Ethics committee of Grenoble University Hospital (CHUGA) and the French Blood Agency's Institutional Review Board Committee (IRB), and declared under the reference #DC-2008-787 (EFS) and collection AC-2017-2949 (CHUGA). Patients gave the written informed consent, and their records were de-identified prior to the analysis. Blinding and randomisation of groups were not relevant to this study. Blood samples were obtained from stage I-IV melanoma patients ( $n = 26$ ) and HDs (HD,  $n = 63$ ) (both sexes). PBMCs were isolated using Ficoll-Hypaque density gradient centrifugation (Eurobio, Les Ulis, France). Lymph node or cutaneous metastatic tumors were obtained from 32 melanoma patients (naïve of treatment by immunotherapies). Tumor samples were reduced to cell suspensions by enzymatic digestion with 2 mg mL<sup>-1</sup> collagenase-D (Roche, Boulogne-Billancourt, France) 20 U mL<sup>-1</sup> DNase (Sigma, Lyon, France) and mechanical disruption. The resulting cell suspensions were filtered and washed. Blood and tumor samples were biobanked and stored in liquid nitrogen at -196°C until use. Patients' clinical features are reported in Supplementary tables 1 (blood samples) and 2 (tumor samples). Progression-free survival and OS were calculated both from diagnosis and sampling times.

### Phenotypic analysis of pDC subsets by multi-parametric flow cytometry

Frozen samples were thawed and stained in PBS 2% fetal calf serum (FCS) with several fluorochrome-labelled anti-human antibodies depending on the analyses. The combination of the following surface markers allowed defining pDCs: CD11c (BD Biosciences, Le Pont de Claix, France: Cat #565227, RRID:AB\_2739122), HLA-DR (BD Biosciences Cat #641411, RRID:AB\_2870307), Lin (BD Biosciences Cat #340546, RRID:AB\_400053), CD45 (BioLegend, Paris, France: Cat #304034, RRID:AB\_2563426), BDCA2 (Miltenyi Biotec, Paris Cat #130-113-190, RRID:AB\_2726015), BDCA4 (Miltenyi Biotec Cat #130-113-515, RRID:AB\_2733317), Axl (Thermo Fisher Scientific, Illkirch, France: Cat #25-1087-42, RRID:AB\_2723959) fluorochrome-labelled anti-human antibody was used to exclude Axl<sup>+</sup> DCs when analysing pDC subsets as well as characterise the Axl<sup>+</sup> DCs in melanoma patients. To depict the four previously described subpopulations of pDCs within the CD45<sup>+</sup> Lin<sup>-</sup> HLA-DR<sup>+</sup> CD11c<sup>-</sup> Axl<sup>-</sup> BDCA2/4<sup>+</sup> pDCs, CD80 (Beckman, Roissy, France) and PDL1 (BD Biosciences Cat #563738, RRID:AB\_2738396) fluorochrome-labelled anti-human antibodies were used. The basal expression of CD2, LAG3 and TRAIL amongst all the pDC subpopulations were also assessed using the corresponding fluorochrome-labelled anti-human

antibody (BD Biosciences Cat #740160, RRID:AB\_2739913, Cat #744727, RRID:AB\_2742438, and Cat #743721, RRID:AB\_2741697 respectively). Anti-CD40 (Beckman) and -CD86 (BD Biosciences Cat #561124, RRID:AB\_10564087) antibodies allowed revealing the basal activation status of each pDC subpopulation. Stained cells were then analysed using LSRII Flow Cytometer and BD FACSDiva Software v.8, RRID:SCR\_001456 (BD). Isotype controls were used to differentiate positive cells from nonspecific background staining (CD45<sup>+</sup> cells containing both negative and positive cells) also served to determine the threshold of positivity). Dead cells were excluded with Live and Dead staining (Thermo Fisher Scientific). To ensure quality control during the study, we performed a standardisation of the fluorescence intensities using cytometer setup and tracking beads (CST) (BD). Samples from all groups were treated similarly, and cell viability was systematically assessed.

## Functional analysis of circulating and tumor-infiltrating pDC subsets in response to TLRs triggering

### Maturation of pDC subsets

To study the maturation of pDCs after TLR-L stimulation, PBMC or tumor-infiltrating cells were cultured in complete RPMI medium at  $4 \times 10^6$  cells mL<sup>-1</sup> for 20 h with or without a single or a mixture of TLR ligands including polyinosinic-polycitidylic acid (polyI:C, TLR3L, 30 µg mL<sup>-1</sup>), Resiquimod (R848, TLR7/8L, 1 µg mL<sup>-1</sup>) and Class-A CpG oligonucleotide ODN-2336 (CpG<sub>A</sub>, TLR9L, 1.5 µM) (Invivogen, Toulouse). pDC subsets were depicted using anti-CD11c, -HLA-DR, -PDL1 (BD), -Lin, -CD45 (Biolegend), -BDCA2 (Miltenyi) and -CD80 (Beckman) Abs. The potential upregulation of the co-stimulatory molecules on pDCs subpopulations was then investigated using the fluorochrome-labelled anti-human CD86 (BD) and CD40 (Beckman) antibodies. Dead cells were excluded with live and dead staining (Thermo Fisher Scientific). Analyses were performed using LSRII Flow Cytometer and BD FACSDiva Software v.8, RRID:SCR\_001456 (BD). (BD).

### TGFβ secretion by tumor infiltrates

Tumor-infiltrating cells were cultured in complete RPMI medium at  $4 \times 10^6$  cells mL<sup>-1</sup> with or without a single or a mixture of TLR ligands including polyinosinic-polycitidylic acid (polyI:C, TLR3L, 30 µg mL<sup>-1</sup>), Resiquimod (R848, TLR7/8L, 1 µg mL<sup>-1</sup>) and Class-A CpG oligonucleotide ODN-2336 (CpG<sub>A</sub>, TLR9L, 1.5 µM) (Invivogen). Culture supernatants were harvested after 20 h culture, and TGFβ cytokine secretion was measured by LUMINEX technology using MAGPIX<sup>®</sup>200 instrument with xPONENT<sup>®</sup> software (Bio-Rad, Cressier, Switzerland).

### Intracellular cytokine staining within pDC subsets and cytotoxic potential evaluation

Cultures were performed in RPMI-1640/GlutaMAX (Invitrogen, Courtaboeuf, France) supplemented with 1% non-essential amino acids, 100 µg mL<sup>-1</sup> gentamycin, 10%

FCS (Invitrogen) and 1 mmol L<sup>-1</sup> sodium pyruvate (Sigma) (complete medium). For intracellular cytokine characterisation, PBMC or tumor infiltrating cells from the different samples were cultured at  $4 \times 10^6$  cells mL<sup>-1</sup> for 5 h, 8 h, 18 h or 24 h with or without TLR ligands alone or mixed together, including polyinosinic-polycitidylic acid (polyI:C, TLR3L, 30 µg mL<sup>-1</sup>), Resiquimod (R848, TLR7/8L, 1 µg mL<sup>-1</sup>), Imiquimod (IMQ, TLR7L, 1 µg mL<sup>-1</sup>), Class-A CpG oligonucleotide ODN-2336 (CpG<sub>A</sub>, TLR9L, 1.5 µM) (Invivogen) and Class-C CpG oligonucleotide ODN-2395 (CpG<sub>C</sub>, TLR9L, 1 µM). Brefeldin A (1 µg mL<sup>-1</sup>) (BD) was added for the last 4 h of culture. Cells were then stained for surface markers allowing to define pDCs (CD45 (Biolegend), HLA-DR (BD), BDCA4 (Miltenyi)). Axl (Invitrogen) fluorochrome-labelled anti-human antibody was used to exclude Axl<sup>+</sup> DCs. The subpopulations of pDCs were delineated using CD80 (Beckman) and PDL1 (BD) fluorochrome-labelled anti-human antibodies. The expression of CD2 and LAG3 amongst pDC subpopulations were also assessed using the corresponding fluorochrome-labelled anti-human antibody (BD). TRAIL (BD Biosciences Cat #743721, RRID:AB\_2741697) allowed assessing the cytotoxic potential of each pDC subpopulation upon TLR stimulation. Cells were then fixed and permeabilised following the manufacturers' instructions (BD). Intracellular cytokine staining was then performed using the fluorochrome-labelled anti-human IL-6 (Biolegend Cat #501118, RRID:AB\_2572040), CXCL-10 (IP-10) (BioTechne, Rennes, France) and IFNα (Miltenyi Biotec Cat #130-116-873, RRID:AB\_2727733) antibodies. Dead cells were excluded with Live and Dead staining (Thermo Fisher Scientific). Analyses were done by flow cytometry using a LSRII Flow Cytometer and BD FACSDiva Software v.8, RRID:SCR\_001456 (BD).

### Statistical analyses

Raw data were analysed in a blinded way. Statistical analyses were performed using the Mann-Whitney non-parametric *U*-test combined with Bonferroni correction, and the Kruskal-Wallis non-parametric test with the post hoc Dunns' test using GraphPad Prism software, RRID:SCR\_002798. The data are shown as means and significance threshold was placed at  $P < 0.05$ . Survival analyses (Cox regression, Kaplan-Meier), correlations, heat maps and PCA were performed using the survival, GGally, gplots, ggplot2 (RRID:SCR\_014601), ggbiplot, MissMDA and FactoMineR (RRID:SCR\_014602) packages of the R i386 software version 3.6.2. Data clustering and global visualisation was performed using Cytobank software (Beckman) and the available analysis algorithms (visNE, FlowSOM).

### ACKNOWLEDGMENTS

We thank Dr D Legrand and her staff at EFS Auvergne Rhone-Alpes for providing healthy volunteers' blood samples. We acknowledge the surgeons and anatomopathology Department from CHU Grenoble Alpes for providing tumor samples especially Dr Nicole Pinel and Pr Nathalie Sturm. We thank Corinne Lucas from the Medical Unit of Molecular genetic of CHU Grenoble Alpes for managing the patients' biobank. We are grateful to Professor B Toussaint, Dr A Legouellec and C Trocme from

TIMC-IMAG-UMR-5525, CHU-Grenoble for access to the Luminex platform; M Pezet, A Grichine and P Marche for access to the cytometry platform; and all the volunteers and patients who agreed to participate in this study.

## CONFLICT OF INTEREST

The authors report no conflict of interest.

## AUTHOR CONTRIBUTIONS

**Eleonora Sosa Cuevas:** Conceptualisation; data curation; formal analysis; investigation; methodology; validation; visualisation; writing – original draft; writing – review and editing. **Nathalie Bendriss-Vermare:** Conceptualisation; investigation; methodology; validation; writing – review and editing. **Stephane Mouret:** Data curation; resources; validation; writing – review and editing. **Florence De Fraipont:** Data curation; resources; validation; writing – review and editing. **Julie Charles:** Conceptualisation; resources; validation; writing – review and editing. **Jenny Valladeau-guilemond:** Conceptualisation; methodology; validation; writing – review and editing. **Laurence Chaperot:** Conceptualisation; funding acquisition; project administration; supervision; validation; writing – review and editing. **Caroline Aspod:** Conceptualisation; formal analysis; funding acquisition; investigation; methodology; project administration; supervision; validation; visualisation; writing – original draft; writing – review and editing.

## REFERENCES

- Banchereau J, Palucka AK. Dendritic cells as therapeutic vaccines against cancer. *Nat Rev Immunol* 2005; **5**: 296–306.
- Steinman RM, Banchereau J. Taking dendritic cells into medicine. *Nature* 2007; **449**: 419–426.
- Chen DS, Mellman I. Oncology meets immunology: the cancer-immunity cycle. *Immunity* 2013; **39**: 1–10.
- Colonna M, Trinchieri G, Liu YJ. Plasmacytoid dendritic cells in immunity. *Nat Immunol* 2004; **5**: 1219–1226.
- Lande R, Gilliet M. Plasmacytoid dendritic cells: key players in the initiation and regulation of immune responses. *Ann NY Acad Sci* 2010; **1183**: 89–103.
- Reizis B. Plasmacytoid dendritic cells: development, regulation, and function. *Immunity* 2019; **50**: 37–50.
- Alcubumbre S, Raieli S, Hoffmann C, Chelbi R, Danlos FX, Soumelis V. Plasmacytoid pre-dendritic cells (pDC): from molecular pathways to function and disease association. *Semin Cell Dev Biol* 2019; **86**: 24–35.
- Zitvogel L, Galluzzi L, Kepp O, Smyth MJ, Kroemer G. Type I interferons in anticancer immunity. *Nat Rev Immunol* 2015; **15**: 405–414.
- Mitchell D, Chintala S, Dey M. Plasmacytoid dendritic cell in immunity and cancer. *J Neuroimmunol* 2018; **322**: 63–73.
- Villadangos JA, Young L. Antigen-presentation properties of plasmacytoid dendritic cells. *Immunity* 2008; **29**: 352–361.
- Tel J, van der Leun AM, Figdor CG, Torensma R, de Vries IJ. Harnessing human plasmacytoid dendritic cells as professional APCs. *Cancer Immunol Immunother* 2012; **61**: 1279–1288.
- Jensen TO, Schmidt H, Moller HJ et al. Intratumoral neutrophils and plasmacytoid dendritic cells indicate poor prognosis and are associated with pSTAT3 expression in AJCC stage I/II melanoma. *Cancer* 2012; **118**: 2476–2485.
- Camisaschi C, De Filippo A, Beretta V et al. Alternative activation of human plasmacytoid DCs *in vitro* and in melanoma lesions: involvement of LAG-3. *J Invest Dermatol* 2014; **134**: 1893–1902.
- Li S, Wu J, Zhu S, Liu YJ, Chen J. Disease-associated plasmacytoid dendritic cells. *Front Immunol* 2017; **8**: 1268.
- Aspod C, Leccia MT, Charles J, Plumas J. Plasmacytoid dendritic cells support melanoma progression by promoting Th2 and regulatory immunity through OX40L and ICOSL. *Cancer Immunol Res* 2013; **1**: 402–415.
- Aspod C, Leccia MT, Charles J, Plumas J. Melanoma hijacks plasmacytoid dendritic cells to promote its own progression. *Oncoimmunology* 2014; **3**: e27402.
- Ito T, Amakawa R, Inaba M et al. Plasmacytoid dendritic cells regulate Th cell responses through OX40 ligand and type I IFNs. *J Immunol* 2004; **172**: 4253–4259.
- Faget J, Bendriss-Vermare N, Gobert M et al. ICOS-ligand expression on plasmacytoid dendritic cells supports breast cancer progression by promoting the accumulation of immunosuppressive CD4<sup>+</sup> T cells. *Cancer Res* 2012; **72**: 6130–6141.
- Sisirak V, Faget J, Gobert M et al. Impaired IFN- $\alpha$  production by plasmacytoid dendritic cells favors regulatory T-cell expansion that may contribute to breast cancer progression. *Cancer Res* 2012; **72**: 5188–5197.
- Sisirak V, Faget J, Vey N et al. Plasmacytoid dendritic cells deficient in IFN $\alpha$  production promote the amplification of FOXP3 regulatory T cells and are associated with poor prognosis in breast cancer patients. *Oncoimmunology* 2013; **2**: e22338.
- Swiecki M, Colonna M. The multifaceted biology of plasmacytoid dendritic cells. *Nat Rev Immunol* 2015; **15**: 471–485.
- Hanahan D, Weinberg RA. Hallmarks of cancer: the next generation. *Cell* 2011; **144**: 646–674.
- Gerlini G, Urso C, Mariotti G et al. Plasmacytoid dendritic cells represent a major dendritic cell subset in sentinel lymph nodes of melanoma patients and accumulate in metastatic nodes. *Clin Immunol* 2007; **125**: 184–193.
- Saadeh D, Kurban M, Abbas O. Plasmacytoid dendritic cell role in cutaneous malignancies. *J Dermatol Sci* 2016; **83**: 3–9.
- Charles J, Chaperot L, Hannani D et al. An innovative plasmacytoid dendritic cell line-based cancer vaccine primes and expands antitumor T-cells in melanoma patients in a first-in-human trial. *Oncoimmunology* 2020; **9**: 1738812.
- Matsui T, Connolly JE, Michnevitz M et al. CD2 distinguishes two subsets of human plasmacytoid dendritic cells with distinct phenotype and functions. *J Immunol* 2009; **182**: 6815–6823.
- Bryant C, Fromm PD, Kupresanin F et al. A CD2 high-expressing stress-resistant human plasmacytoid dendritic-cell subset. *Immunol Cell Biol* 2016; **94**: 447–457.

28. Zhang H, Gregorio JD, Iwahori T *et al.* A distinct subset of plasmacytoid dendritic cells induces activation and differentiation of B and T lymphocytes. *Proc Natl Acad Sci USA* 2017; **114**: 1988–1993.
29. Musumeci A, Lutz K, Winheim E, Krug AB. What makes a pDC: recent advances in understanding plasmacytoid DC development and heterogeneity. *Front Immunol* 2019; **10**: 1222.
30. Marsman C, Lafouresse F, Liao Y *et al.* Plasmacytoid dendritic cell heterogeneity is defined by CXCL10 expression following TLR7 stimulation. *Immunol Cell Biol* 2018; **96**: 1083–1094.
31. Bjorck P, Leong HX, Engleman EG. Plasmacytoid dendritic cell dichotomy: identification of IFN- $\alpha$  producing cells as a phenotypically and functionally distinct subset. *J Immunol* 2011; **186**: 1477–1485.
32. Villani AC, Satija R, Reynolds G *et al.* Single-cell RNA-seq reveals new types of human blood dendritic cells, monocytes, and progenitors. *Science* 2017; **356**: eaah4573.
33. Alcantara-Hernandez M, Leylek R, Wagar LE *et al.* High-dimensional phenotypic mapping of human dendritic cells reveals interindividual variation and tissue specialization. *Immunity* 2017; **47**(6): 1037–1050.e6.
34. Collin M, Bigley V. Human dendritic cell subsets: an update. *Immunology* 2018; **154**: 3–20.
35. Leylek R, Alcantara-Hernandez M, Lanzar Z *et al.* Integrated cross-species analysis identifies a conserved transitional dendritic cell population. *Cell Rep* 2019; **29**: 3736–3750.e8.
36. Chen YL, Gomes T, Hardman CS *et al.* Re-evaluation of human BDCA-2<sup>+</sup> DC during acute sterile skin inflammation. *J Exp Med* 2020; **217**: jem.20190811.
37. Du Q, Jiao Y, Hua W *et al.* Preferential depletion of CD2<sup>low</sup> plasmacytoid dendritic cells in HIV-infected subjects. *Cell Mol Immunol* 2011; **8**: 441–444.
38. Alcumbre SG, Saint-Andre V, Di Domizio J *et al.* Diversification of human plasmacytoid predendritic cells in response to a single stimulus. *Nat Immunol* 2018; **19**: 63–75.
39. Onodi F, Bonnet-Madin L, Meertens L *et al.* SARS-CoV-2 induces human plasmacytoid predendritic cell diversification via UNC93B and IRAK4. *J Exp Med* 2021; **218**: e20201387.
40. Sosa Cuevas E, Ouaguia L, Mouret S *et al.* BDCA1<sup>+</sup> cDC2s, BDCA2<sup>+</sup> pDCs and BDCA3<sup>+</sup> cDC1s reveal distinct pathophysiologic features and impact on clinical outcomes in melanoma patients. *Clin Transl Immunol* 2020; **9**: e1190.
41. Girard P, Sosa Cuevas E, Ponsard B *et al.* Dysfunctional BTN3A together with deregulated immune checkpoints and type I/II IFN dictate defective interplay between pDCs and  $\gamma\delta$  T cells in melanoma patients, which impacts clinical outcomes. *Clin Transl Immunol* 2021; **10**: e1329.
42. Rapp M, Wintergerst MWM, Kunz WG *et al.* CCL22 controls immunity by promoting regulatory T cell communication with dendritic cells in lymph nodes. *J Exp Med* 2019; **216**: 1170–1181.
43. Faget J, Biota C, Bachelot T *et al.* Early detection of tumor cells by innate immune cells leads to T<sub>reg</sub> recruitment through CCL22 production by tumor cells. *Cancer Res* 2011; **71**: 6143–6152.
44. Galluzzi L, Buque A, Kepp O, Zitvogel L, Kroemer G. Immunogenic cell death in cancer and infectious disease. *Nat Rev Immunol* 2017; **17**: 97–111.
45. Paijo J, Doring M, Spanier J *et al.* cGAS senses human cytomegalovirus and induces type I interferon responses in human monocyte-derived cells. *PLoS Pathog* 2016; **12**: e1005546.
46. Lande R, Gregorio J, Facchinetti V *et al.* Plasmacytoid dendritic cells sense self-DNA coupled with antimicrobial peptide. *Nature* 2007; **449**: 564–569.
47. Ganguly D, Chamilos G, Lande R *et al.* Self-RNA-antimicrobial peptide complexes activate human dendritic cells through TLR7 and TLR8. *J Exp Med* 2009; **206**: 1983–1994.
48. Ries M, Schuster P, Thomann S, Donhauser N, Vollmer J, Schmidt B. Identification of novel oligonucleotides from mitochondrial DNA that spontaneously induce plasmacytoid dendritic cell activation. *J Leukoc Biol* 2013; **94**: 123–135.
49. Shen JX, Liu J, Zhang GJ. Interleukin-33 in malignancies: friends or foes? *Front Immunol* 2018; **9**: 3051.
50. Stary G, Bangert C, Tauber M, Strohal R, Kopp T, Stingl G. Tumoricidal activity of TLR7/8-activated inflammatory dendritic cells. *J Exp Med* 2007; **204**: 1441–1451.
51. Chaperot L, Blum A, Manches O *et al.* Virus or TLR agonists induce TRAIL-mediated cytotoxic activity of plasmacytoid dendritic cells. *J Immunol* 2006; **176**: 248–255.

## Supporting Information

Additional supporting information may be found online in the Supporting Information section at the end of the article.



This is an open access article under the terms of the Creative Commons Attribution-NonCommercial-NoDeriv License, which permits use and distribution in any medium, provided the original work is properly cited, the use is non-commercial and no modifications or adaptations are made.